

# Protein tyrosine phosphatase L1 inhibits high-grade serous ovarian carcinoma progression by targeting I $\kappa$ B $\alpha$

Yacheng Wang

Miao Li

Ting Huang

Jun Li

Department of Oncology, The Central Hospital of Wuhan, Wuhan, Hubei, China

**Background:** High-grade serous ovarian cancer (HGSOC) represents most of the ovarian cancers and accounts for 70%–80 % of related deaths. The overall survival of HGSOC has not been remarkably improved in the past decades, due to the tumor dissemination in peritoneal cavity and invasion of adjacent organs. Therefore, identifying molecular biomarkers is invaluable in helping predicting clinical outcomes and developing targeted chemotherapies. Although there have been studies revealing the prognostic significance of protein tyrosine phosphatase L1 (PTPL1) in breast cancer and lung cancer, its involvement and functions in HGSOC remains to be elucidated.

**Methods:** We retrospectively enrolled a cohort of HGSOC patients after surgical resection. And analyzed the mRNA and protein levels of PTPL1 in tissue samples.

**Results:** We found that PTPL1 presented a lower expression in HGSOC tissues than in adjacent normal ovarian tissues. Besides, the PTPL1 level was negatively correlated with tumor stage, implying its potential role as a tumor suppressor. Univariate and multivariate analyses identified that patients with higher PTPL1 showed a better overall survival compared to those with lower PTPL1 expression. In addition, cellular experiments confirmed the role of PTPL1 in suppressing tumor proliferation and invasion. Furthermore, we demonstrated that PTPL1 negatively regulated phosphorylation of tyrosine 42 on I $\kappa$ B $\alpha$  (I $\kappa$ B $\alpha$ -pY42). To our knowledge, this is the initial finding on PTPL1 targeting I $\kappa$ B $\alpha$ -pY42 site. Finally, our data indicated that PTPL1 suppressed tumor progression by dephosphorylating I $\kappa$ B $\alpha$ -pY42, which stabilized I $\kappa$ B $\alpha$  and attenuated nucleus translocation of NF- $\kappa$ B.

**Conclusion:** Our study revealed a tumor-suppressing role of PTPL1 in HGSOC by targeting I $\kappa$ B $\alpha$ .

**Keywords:** I $\kappa$ B $\alpha$ , phosphorylation, prognosis, PTPL1, serous ovarian carcinoma, overall survival

## Introduction

Epithelial ovarian cancer is the most lethal gynecologic malignancy,<sup>1</sup> and high-grade serous ovarian carcinoma (HGSOC) accounts for most of the morbidity and mortality in this tumor type. Although the concept of HGSOC has been raised up for decades, till now, our understanding of HGSOC remains limited compared with other tumor types.<sup>2</sup> HGSOC is generally diagnosed at advanced FIGO stages (stage III and stage IV), and the accurate diagnosis of this specific histological tumor type was only established in the last decade. Interestingly, the origin of HGSOC is the fallopian tubes instead of ovarian tissues.<sup>3</sup> The poor prognosis of HGSOC is partially resulted from lacking early disease-specific symptoms and biomarkers. For example, the cancer antigen 125 (CA-125) is useful in monitoring disease status but failed to accomplish detection of early FIGO stage.<sup>4</sup>

Correspondence: Jun Li  
Department of Oncology, The Central Hospital of Wuhan, No 26 Shengli Road, Jiangan District, Wuhan, Hubei 430014, China  
Tel +86 27 6569 6508  
Email [vinvali\\_edu@163.com](mailto:vinvali_edu@163.com)

In addition, HGSOC is initially hypersensitive to platinum chemotherapy, however, up to 75% of those responding cases occur with platinum-resistant relapse, and the 5-year survival rate is less than 40%.<sup>5</sup> Last but not least, HGSOC is characterized with high invasive capacity, and the underlying molecular mechanism is still the major limitation for developing novel therapies. Therefore, identifying novel and reliable biomarkers for early diagnosis of HGSOC is urgently needed.<sup>6</sup>

Phosphorylation and de-phosphorylation are one of the most important post-translational modifications in functional proteins.<sup>7</sup> Tyrosine phosphorylation is balanced by various kinases and protein tyrosine phosphatases (PTPs), playing critical roles in cellular survival, proliferation, and motility. PTPL1, also known as PTPN13, is a kind of non-receptor PTPs.<sup>8</sup> Besides the conserved PTP domain for catalyzing de-phosphorylation, PTPL1 contains complex interaction domains such as PDZ domains.<sup>9</sup> Due to the diversity of protein substrates, PTPL1 may show distinct roles in different tumor types. For example, PTPL1 can dephosphorylate insulin receptor substrate-1 (IRS-1) and induce apoptosis of HeLa cells.<sup>10</sup> In contrast, PTPL1 dephosphorylates Fas (Apo-1, CD95) protein, subsequently suppresses the Fas-caspase 8 apoptosis signaling pathway and promotes tumor progression of hepatocellular carcinoma.<sup>11</sup> Therefore, identifying novel PTPL1 substrates will significantly enlarge our understanding of the molecular basis for its distinct functions in tumors.

PTPL1 has been reported to be upregulated in Fas-resistant ovarian cancer cell line SKOV3 and induced chemoresistance by downregulating the Fas protein.<sup>12</sup> However, its prognostic role in HGSOC patients has not been systematically studied. In this study, we explored the mRNA and protein expression of PTPL1 in clinical HGSOC samples and identified that its lower expression is an unfavorable prognostic factor. In addition, we found that PTPL1 can directly inhibit proliferation and invasion of HGSOC cells, which is completely different from the results in chemoresistant cell lines.<sup>12</sup> Furthermore, our data revealed  $\text{I}\kappa\text{B}\alpha$  (nuclear factor of kappa light polypeptide gene enhancer in B-cells inhibitor, alpha) as a novel substrate of PTPL1.

## Patients and methods

### Patients and samples

Formalin-fixed, paraffin-embedded HGSOC tissues (n=97, the median patient age was 64.0 years) were collected from the Central Hospital of Wuhan (2009–2017). Patients' information including age, pathological grade, FIGO stage, and serum CA-125 levels at the time of diagnosis were retrieved. The median follow-up time for our cohort was

42 months, ranging 9–89 months. Another seven paired HGSOC tissues and adjacent nontumorous ovarian tissues were stored in  $-80^{\circ}\text{C}$  immediately after surgical resection. None of the patients underwent preoperative chemotherapy or radiotherapy. After surgery, 37 (37/97, 38.1%) patients received only paclitaxel chemotherapy, 49 (49/97, 50.5%) patients were treated with paclitaxel and carboplatin, and the other 11 (11/97, 11.3%) patients were treated with platinum and cyclophosphamide. All the patients underwent R0 resection, and final diagnoses were based on histological and pathological examinations.<sup>13</sup> The accurate diagnosis of HGSOC was based on histological examination, p53 test, and WT1 (Wilms' tumor 1) test. Mutate p53 was used to distinguish HGSOC with LGSOC, while WT1 was used to distinguish HGSOC with endometrioid carcinoma.<sup>2</sup> Research use of tissue samples was approved by the ethical committee of the Central Hospital of Wuhan. Signed informed consents were obtained from all the cases enrolled in this study.

### Quantitative real-time polymerase chain reaction

Total RNA was extracted from fresh frozen tissue samples with TRIzol reagent (Thermo Fisher Scientific, Waltham, MA, USA) according to the manufacturer's instructions. The concentration and purity of isolated RNA were confirmed by a NanoDrop instrument (NanoDrop Technologies, Wilmington, DE, USA). cDNA was generated by reverse transcription from 1  $\mu\text{g}$  RNA using a Superscript III kit (Thermo Fisher Scientific). qPCR analysis was then performed to evaluate the mRNA level of *PTPL1* in HGSOC and adjacent nontumorous tissues. The *PTPL1* primers were designated as 5'-GCGAAATGATCAGTTGCCAATAG-3' and 5'-ACTTGGCACCCGTCTATTTACC-3'.<sup>14</sup> In addition, housekeeping gene *GAPDH* was used as internal control to normalize the variability in different groups (primers: 5'-GCCGC ATCTTCTTTTTCGTCGC-3' and 5'-TCCCGTTCTCAGCCTTGACGGT-3').<sup>15</sup> Transcription levels were calculated using the  $2^{-\Delta\Delta\text{Ct}}$  method.<sup>16</sup> All experiments were performed in triplicate for at least three times.

### Western blot

Immunoblotting assays were performed to evaluate the expression or phosphorylation levels of various proteins. Fresh-frozen tissues or harvested cells were homogenized in RIPA buffer to generate total cell lysates. Nucleus fraction was isolated as described by others.<sup>17</sup> Total protein concentration was measured using a BCA Protein Assay Kit (Pierce, Rockford, IL, USA). Briefly, 20  $\mu\text{g}$  of total proteins was resolved on

10% SDS/PAGE gels, transferred onto polyvinylidene fluoride membranes (EMD Millipore, Billerica, MA), blocked with 5% nonfat milk, and probed with primary antibodies including PTPL1, I $\kappa$ B $\alpha$ , phospho-I $\kappa$ B $\alpha$  (Tyr42), NF- $\kappa$ B, caspase 3, caspase 9, and  $\beta$ -actin (Santa Cruz Biotechnology Inc., Dallas, TX, USA). Horseradish peroxidase-conjugated secondary antibodies were then incubated for 1 hour at room temperature followed by detection with enhanced chemiluminescence solution (Thermo Fisher Scientific).

## Immunohistochemistry (IHC) and IHC evaluation

Formalin-fixed, paraffin-embedded HGSOc tissues were cut into 4  $\mu$ m sections, followed by de-paraffinized and re-hydrated. After antigen retrieval in a microwave for 10 minutes, sections were blocked with non-immunoreactivity goat serum and then incubated overnight with anti-PTPL1 (Abcam, Cat No ab198882, 1:100 dilution) or anti-phospho-I $\kappa$ B $\alpha$ -Y42 (Abcam, Cat No ab24783; Cambridge, MA, USA; 1:100 dilution) antibodies at 4°C. Negative controls were conducted by incubating with PBS instead of primary antibody. Sections were then incubated with the corresponding biotinylated secondary antibody at room temperature for 2 hours. Immunoreactivity was visualized with 3,3-diaminobenzidine (DAB) staining for 15 minutes. The slides were finally counterstained with 1% hematoxylin and evaluated by two independent pathologists. As described by others,<sup>15</sup> PTPL1 expressions were scored by determining the percentage and staining intensity of positive cells in three different visual fields at  $\times$ 100 magnification. The percentage of positive tumor cells was scored as follows: 0 (0%–10%), 1 (11%–50%), 2 (51%–75%), and 3 (75%–100%).<sup>18</sup> The staining intensity was graded into 0 (negative), 1 (weakly positive), 2 (moderately positive), and 3 (strongly positive). The final IHC score of PTPL1 was weighted by multiplying the intensity and percentage scores (range 0–9).<sup>19</sup> High PTPL1 immunostaining was defined as IHC score  $\geq$ 4, while  $<$ 4 was defined as a low PTPL1 expression.

## Cell culture and transfection

The human high-grade serous ovarian carcinoma cell line OV-90 was obtained from the China Center for Type Culture Collection (CCTCC, Wuhan, Hubei, China). Primary ovarian cancer (POC) cells were established following the procedures described by others,<sup>20</sup> and human normal fallopian tube epithelium cells (FTEC) were purchased from Lifeline Cell Technology (Carlsbad, CA, USA) (Cat. No FC-0081). All cells were maintained in DMEM supplemented with 10% FBS

and 1% penicillin (10,000 U/mL)/streptomycin (10 mg/mL) in a humidified atmosphere at 37°C with 5% CO<sub>2</sub>.

The coding regions of PTPL1 were cloned into a pCMV6 vector (pCMV6-PTPL1). After the confirmation by DNA-Sequencing, pCMV6-PTPL1 was transfected into OV-90 cells to generate PTPL1-overexpressing cells. Knockdown of PTPL1 was achieved using an siRNA with the following sequence: 5'-CAGAUCAGCUUCCUGUAA-3' (position 1,028–1,046). Both overexpression and siRNA-knockdown were performed with Lipofectamine 2000 reagent (Thermo Fisher Scientific) following the manufacturer's procedure. For each transfection assay, the plasmid construct vector and scrambled siRNA were used as negative control. The transfection efficiencies were tested by Western blot analyses.

## MTT assay

Transfected cells were seeded into 96-well plates ( $5.0 \times 10^3$  cells/well) with a final volume of 150  $\mu$ L/well. At designated time points (day 1, 2, 3, and 4), 20  $\mu$ L MTT solution was added into each well. After another 4 hours incubation at 37°C, the culturing medium was discarded, and crystals were resolved by adding 150  $\mu$ L of DMSO.<sup>21</sup> Cell viability was then assessed by measuring the absorbance at 490 nm wavelength with a 96-well plate reader. All experiments were performed for three times in triplicate.

## Matrigel-transwell assay

Transfected cells within the log phase were resuspended in FBS-free medium and seeded ( $8 \times 10^4$  cells/well) into 24-well Transwell chambers (Corning Incorporated, Corning, NY, USA) pre-coated with Matrigel (Biosciences, San Jose, CA, USA). Medium containing 20% FBS was added into the lower chamber as a chemoattractant. After keeping the culture at 37°C for 48 hours, the invaded cells adhesive to the lower membrane surface were fixed with 100% methanol, stained with 0.5% crystal violet, and counted under a light microscope to determine the average number of cells from five visual fields.<sup>22</sup> Assays were performed in triplicate for three times.

## Statistics

Statistical analysis was performed using the SPSS 18.0 software. Data were expressed as mean  $\pm$  SD. Differences between the two subgroups were evaluated with two-sided chi-squared test. Overall survival time was defined as the period from the date of surgery to the date of death or last follow-up. Univariate analysis was performed using the Kaplan–Meier method and the log-rank test. Parameters with significant prognostic value in the univariate analysis were

subjected to the multivariate Cox regression model to determine their independent role in clinical outcomes. Statistical differences between cellular treatment groups were evaluated by two-tailed Student's *t*-test compared with the control group.  $P < 0.05$  was considered statistically significant.

## Results

### Patients' characteristics

A total number of 97 patients suffered from HGSOc were enrolled in this retrospective study. The median age at the time of diagnosis was 64.0 years. Most of the patients (85/97, 87.6%) were diagnosed with a higher level of serum CA-125 ( $>35$  U/mL), only 12 patients within the normal range of CA-125 (0–35 U/mL). According to the pathological examination, 69 patients were classified as differential grade 3, and the other 28 patients suffered with grade 1–2. Consistent with previous studies, most of the HGSOc patients were with advanced FIGO stage, and only six patients (6/97, 6.2%) were with FIGO stage I or stage II. The median survival time was 42.0 months, and the 5-year overall survival was 32.7%. The detailed clinicopathologic characteristics are listed in Table 1.

### PTPL1 shows lower expression in HGSOc and correlated with disease progression

First, we compared the mRNA levels of *PTPL1* in seven paired HGSOc and adjacent non-tumorous tissues and found that *PTPL1* transcripts were significantly lower in HGSOc

than that in adjacent tissues ( $P=0.042$ , Figure 1A). The protein expression pattern of PTPL1 from fresh-frozen tissues was consistent with that of mRNA, showing a decreased level in tumor tissues (Figure 1B). The results indicated that PTPL1 might play tumor suppressing roles in HGSOc, and we next expanded the case numbers by collecting paraffin-embedded HGSOc tissue samples from the Department of Pathology in our hospital. After excluding those lost to follow-up, the cohort finally contains 97 cases. Most of the adjacent normal ovarian tissues showed strong positive expression of PTPL1 (Figure 1C) in the cytoplasm, while 36 patients (36/97, 37.1%) were identified as a PTPL1 low expression or negative expression in HGSOc tissues (Figure 1D).

By quantifying the PTPL1 staining in HGSOc tissues, all the patients were divided into two groups: low PTPL1 expression group ( $n=36$ ) and high PTPL1 expression group ( $n=61$ ). The associations of PTPL1 expression with different clinicopathological parameters were assessed using the chi-squared test (Table 1). There was no significant difference in patients' age or pathological grade between these two groups ( $P=0.908$  and  $P=0.519$ , respectively). However, PTPL1 level in tumor cells was significantly correlated with the clinical stage ( $P=0.006$ ), on that the HGSOc tissues with advanced clinical stages (III–IV) showed lower PTPL1 expressions than those with early clinical stages (I–II). Interestingly, patients with higher CA-125 levels exhibited significantly higher PTPL1 ( $P=0.027$ ) although the bias is non-negligible due to limited case numbers.

### Decreased PTPL1 indicates poor prognosis of HGSOc patients

Kaplan–Meier survival analyses were then performed to determine the clinical significance of variables (Figure 2). As expected, the advanced FIGO stage was negatively correlated with the poor overall survival ( $P=0.004$ , Table 2). Interestingly, patients with low PTPL1 expression also showed a shorter mean overall survival time compared to those with higher PTPL1 level ( $48.3 \pm 4.1$  vs  $59.5 \pm 3.6$  months,  $P=0.042$ ). Therefore, lower PTPL1 was an unfavorable prognostic factor for the overall survival of HGSOc patients.

Cox proportional-hazard analysis was conducted to further evaluate the independent impact of prognostic factors (Table 3). Accordingly, advanced FIGO stages were statistically significant in predicting a poor clinical outcome ( $HR=2.380$ , 95% CI 1.253–4.522,  $P=0.008$ ). Similarly, the PTPL1 was also found to be an independent prognostic biomarker ( $HR=0.621$ , 95% CI 0.351–0.844,  $P=0.039$ ).

**Table 1** Clinical characteristics of HGSOc patients

Variable	Cases	PTPL1 protein level		P-value
	(n=97)	Low (n=36)	High (n=61)	
<b>Age (years)</b>				0.908
≤60.0	37	14	23	
>60.0	60	22	38	
<b>Pathological grade</b>				0.519
Grade 1–2	28	9	19	
Grade 3	69	27	42	
<b>FIGO stage</b>				0.006*
Stage I–II	6	1	5	
Stage III	72	22	50	
Stage IV	19	13	6	
<b>CA-125 (U/mL)</b>				0.027*
≤35	12	1	11	
>35	85	35	50	

Note: \* $p < 0.05$ .

Abbreviations: CA-125, cancer antigen 125; HGSOc, high-grade serous ovarian cancer; PTPL1, protein tyrosine phosphatase L1.

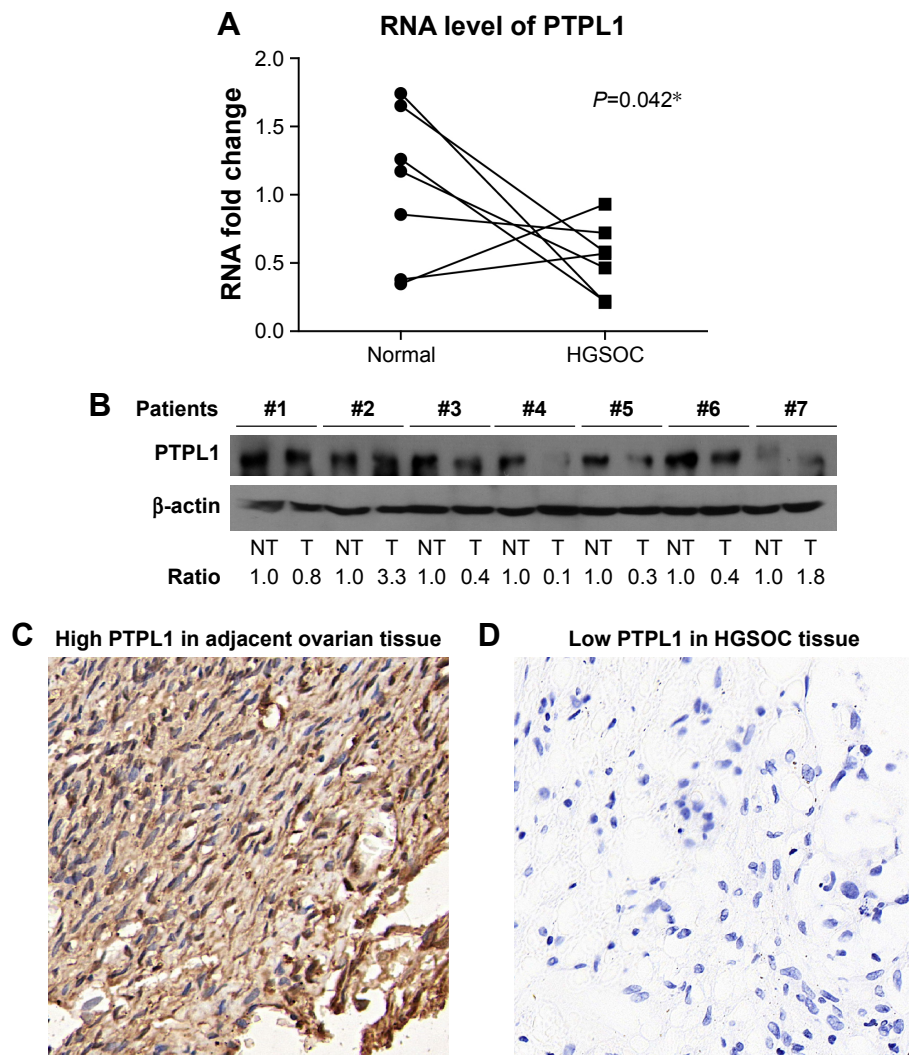


**Figure 1** Expression patterns and cellular localization of PTPL1 in ovarian carcinoma tissues and normal ovarian tissues.

**Notes:** (A) The mRNA level of PTPL1 in HGSOC was significantly lower than that in adjacent NT tissues ( $P=0.042$ ). (B) The protein expression of PTPL1 was compared in seven paired fresh-frozen HGSOC (T) and NT tissues by Western blot, five of them (5/7, 71.4%) showed higher levels in adjacent tissues. (C) Representative images of positive PTPL1 immunohistochemical staining in adjacent ovarian tissues, showing the localization of PTPL1 in the cell cytoplasm. (D) Representative negative-staining images were demonstrated in HGSOC tissues. Magnification:  $\times 400$ .  $*P < 0.05$ .

**Abbreviations:** HGSOC, high-grade serous ovarian cancer; NT, nontumorous; PTPL1, protein tyrosine phosphatase L1.

## PTPL1 inhibits proliferation and invasion of OV-90 cells

To determine the underlying mechanisms of PTPL1 in suppressing tumor progression, we obtained the normal FTEC and the primary serous ovarian cancer (POC) cells. Western blotting results showed a comparable level of PTPL1 protein expression between POC cells and OV-90 ovarian cancer cell line, both significantly lower than that in FTEC cells (Figure 3A). Therefore, we used the OV-90 cell line as the experimental model to explore the cellular effects of PTPL1 on HGSOC. The pCMV6-PTPL1 plasmids and PTPL1-siRNA were transfected into OV-90 cells, respectively. We then investigated the changes in cell proliferation and invasion

capacities. MTT assay demonstrated that overexpressing PTPL1 significantly inhibited OV-90 cell growth, while siPTPL1 promoted cell proliferation (Figure 3B). Similarly, there was a significant decrease in cell invasion in PTPL1-overexpressing cells, whereby the invasion was enhanced in PTPL1-silencing cells compared with the scramble group (Figure 3C).

## PTPL1 suppresses tumor progression by dephosphorylating I $\kappa$ B $\alpha$

Since PTPL1 is a phosphatase, we hypothesized that it may function through dephosphorylating downstream proteins. I $\kappa$ B $\alpha$  is an important cellular protein in modulating the

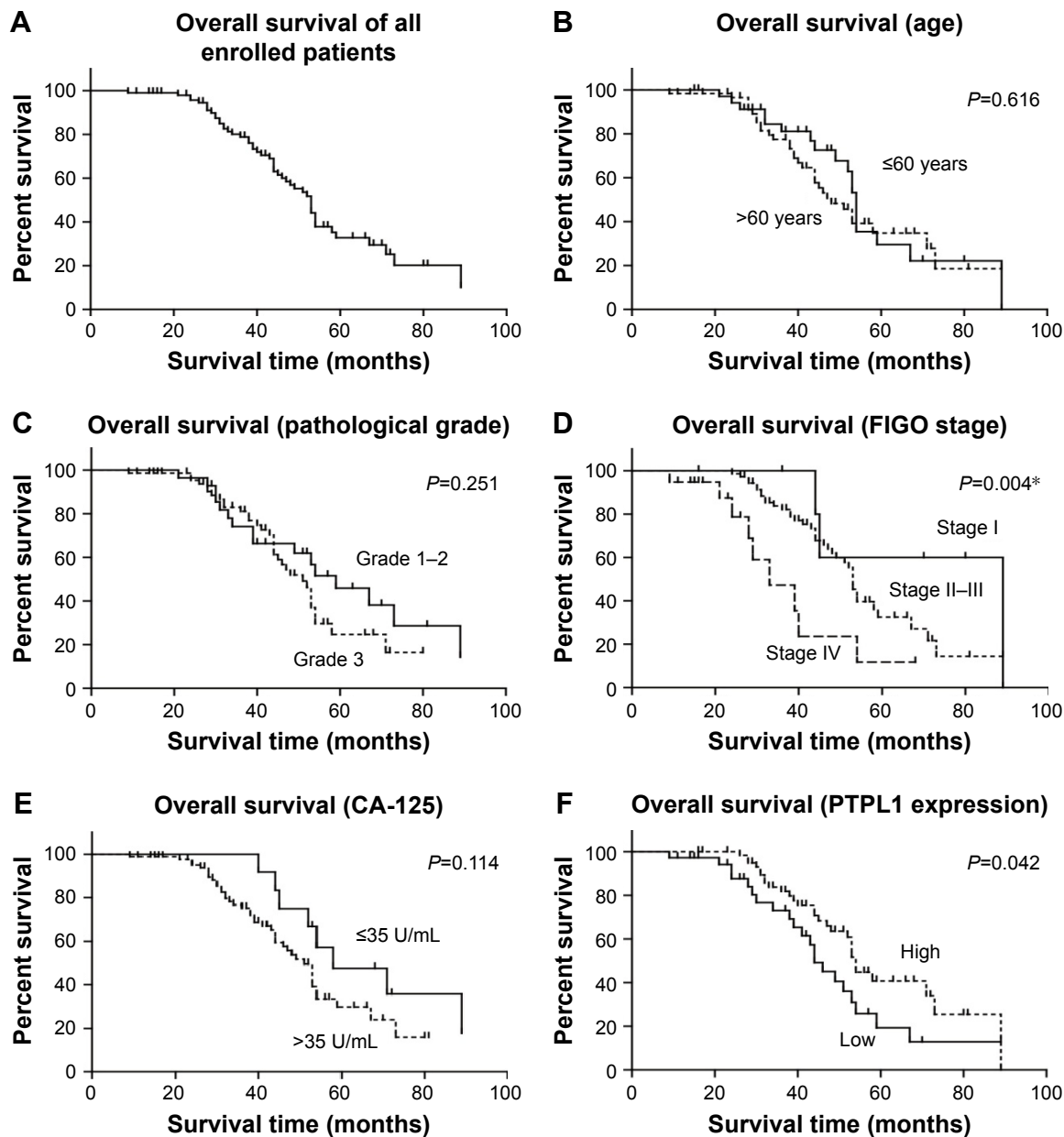


**Figure 2** Kaplan-Meier survival analysis of overall survival according to clinicopathological characteristics.

**Notes:** The overall survival curve of our enrolled cohort was shown (A). Patients' age (B) and pathological grade (C) had no prognostic significance. Patients with advanced FIGO stages (D) and lower CA-125 levels (E) showed better overall survival. In addition, lower PTPL1 protein expression level was identified as an unfavorable prognostic factor by univariate analysis (F). \* $p < 0.05$ .

**Abbreviations:** CA-125, cancer antigen 125; PTPL1, protein tyrosine phosphatase L1.

functions of transcription factor NF- $\kappa$ B (nuclear factor kappa-light-chain-enhancer of activated B cells). In normal conditions, I $\kappa$ B $\alpha$  interacts with NF- $\kappa$ B and prevents its nucleus translocation.<sup>23</sup> Upon phosphorylation, I $\kappa$ B $\alpha$  is quickly degraded, the NF- $\kappa$ B is subsequently released and transports into the nucleus, inducing enhanced transcription.<sup>24</sup> Interestingly, we found that the phosphorylation of I $\kappa$ B $\alpha$  on its tyrosine 42 site (I $\kappa$ B $\alpha$ -pY42) was significantly increased in accordance to tumor stages and showed negative statistical correlation with PTPL1 expression level

(Figure 4A). Furthermore, in the cells transfected with PTPL1, the level of I $\kappa$ B $\alpha$ -pY42 was decreased. In contrast, upon silencing PTPL1 by siRNA, the phosphorylation of I $\kappa$ B $\alpha$ -Y42 was increased while the total I $\kappa$ B $\alpha$  was down-regulated (Figure 4B). The reduced total I $\kappa$ B $\alpha$  protein can be explained by the fact that I $\kappa$ B $\alpha$  phosphorylation will induce its ubiquitination and proteasome degradation.<sup>25</sup> In addition, the nucleus level of NF- $\kappa$ B was negatively regulated by PTPL1, without significant NF- $\kappa$ B alteration in total lysates (Figure 4B). Consistently, caspase protein

**Table 2** Kaplan–Meier estimated overall survival of HGSOc patients

Variable	Cases (n=97)	Overall survival	5-year	P-value
		(months) Mean $\pm$ SD	overall survival	
<b>Age (years)</b>				0.616
$\leq 60.0$	37	56.9 $\pm$ 4.4	29.5%	
$>60.0$	60	54.4 $\pm$ 3.5	34.8%	
<b>Pathological grade</b>				0.251
Grade 1–2	28	59.4 $\pm$ 5.0	45.8%	
Grade 3	69	51.5 $\pm$ 2.7	24.7%	
<b>FIGO stage</b>				0.004*
Stage I–II	6	71.2 $\pm$ 11.9	60.0%	
Stage III	72	55.6 $\pm$ 2.9	32.5%	
Stage IV	19	37.3 $\pm$ 4.7	11.8%	
<b>CA-125 (U/mL)</b>				0.114
$\leq 35$	12	66.0 $\pm$ 6.1	47.6%	
$>35$	85	51.7 $\pm$ 2.6	29.8%	
<b>PTPL1 expression</b>				0.042*
Low	36	48.3 $\pm$ 4.1	25.8%	
High	61	59.5 $\pm$ 3.6	40.7%	

Note: \* $p < 0.05$ .

Abbreviations: CA-125, cancer antigen 125; HGSOc, high-grade serous ovarian cancer; PTPL1, protein tyrosine phosphatase L1.

cleavage was also enhanced by silencing PTPL1, indicating its role in suppressing tumor cell viability.

Because I $\kappa$ B $\alpha$ -pY42 was obviously dephosphorylated by PTPL1, we then aimed to confirm whether PTPL1 suppressed tumor progression through the I $\kappa$ B $\alpha$  signaling pathway. We used a specific I $\kappa$ B $\alpha$  inhibitor, Bay 11-7085, to inhibit its phosphorylation. MTT and Transwell assays indicated that the tumor-promoting effects of PTPL1-siRNA were significantly attenuated by I $\kappa$ B $\alpha$  phosphorylation inhibitor (Figure 4C and D). In order to test the specific effects of Y42 site, we mutated the tyrosine into alanine (Y42A) and co-transfected I $\kappa$ B $\alpha$ -Y42A mutant with PTPL1-siRNA. Proliferation assay identified a comparable effect of Bay 11-7085 inhibitor with I $\kappa$ B $\alpha$ -Y42A overexpression (Figure 4C). Similarly, the cell invasion process was restrained by overexpressing I $\kappa$ B $\alpha$ -Y42A (Figure 4D). Taken together, we put forward the signaling axis of the PTPL1-I $\kappa$ B $\alpha$ -pY42-NF- $\kappa$ B pathway in HGSOc progression (Figure 4E).

## Discussion

In the past decades, studies suggested that kinases and phosphatases are key players in regulating numerous cellular

**Table 3** Cox regression analysis for independent prognostic factors of HGSOc patients

Variable	P-value	HR	95% CI	
			Lower	Upper
FIGO stage	0.008*	2.380	1.253	4.522
PTPL1 expression	0.039*	0.621	0.351	0.844

Note: \* $p < 0.05$ .

Abbreviations: HGSOc, high-grade serous ovarian cancer; PTPL1, protein tyrosine phosphatase L1.

pathways. In this study, we focused on PTPL1, one of the non-receptor tyrosine phosphatases. Several groups have reported that abnormal expression of PTPL1 is involved in malignancies. However, it is still under debate whether PTPL1 is a tumor suppressor or a tumor promoter. Furthermore, PTPL1 showed tumor-suppressing functions in breast cancer and non-small-cell lung cancer.<sup>26,27</sup> In contrast, PTPL1 can protect the pancreatic carcinoma cells from CD95-mediated apoptosis.<sup>28</sup> PTPL1 was also reported to induce chemoresistance of head and neck cancers.<sup>29</sup> To date, the roles of PTPL1 in the progression of ovarian cancer have not yet be fully elucidated.

Here, we found that PTPL1 showed distinct expression patterns in different high-grade serous ovarian cancer (HGSOc) patients. Clinical data suggested that a lower PTPL1 expression in HGSOc tissues was correlated with advanced tumor stage. We then identified PTPL1 as an unfavorable prognostic biomarker for overall survival of HGSOc patients by univariate and multivariate analyses. Interestingly, PTPL1 high expression was previously reported to induce Fas-resistance in ovarian cancer cell lines and maintain cell viability,<sup>12</sup> which is a little different with our findings. However, their results were mainly obtained from cells treated with anti-Fas antibody, an inducer of cell apoptosis. Actually, whether an enzyme acts as an oncogenic molecular or tumor suppressor depends on its cellular localization and substrate targets. In the current study, we identified I $\kappa$ B $\alpha$  as a novel substrate targeted by PTPL1. By inhibitor treatment and site-directed mutagenesis, we confirmed that I $\kappa$ B $\alpha$  phosphorylation on tyrosine 42 was a

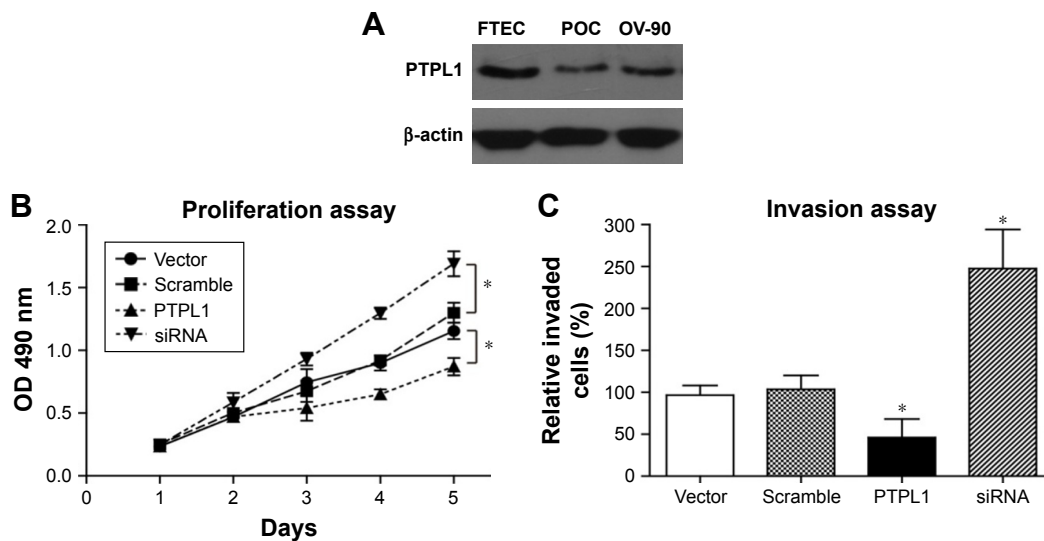


**Figure 3** Effects of PTPL1 on tumor cell proliferation and invasion.

**Notes:** (A) PTPL1 showed detectable expression level in both POC cells and OV-90 cells, although significantly lower than that in normal FTEC. (B) MTT assay revealed a tumor-promoting effect of silencing PTPL1, whereas PTPL1 overexpression attenuated cell proliferation. (C) Transfected OV-90 cells were subjected to Matrigel-Transwell assay, and an approximately 70% decrease was observed in PTPL1-overexpressing cells. Data are presented as mean  $\pm$  SD. \* $P < 0.05$ .

**Abbreviations:** FTEC, fallopian tube epithelium cells; POC, primary ovarian cancer; PTPL1, protein tyrosine phosphatase L1.

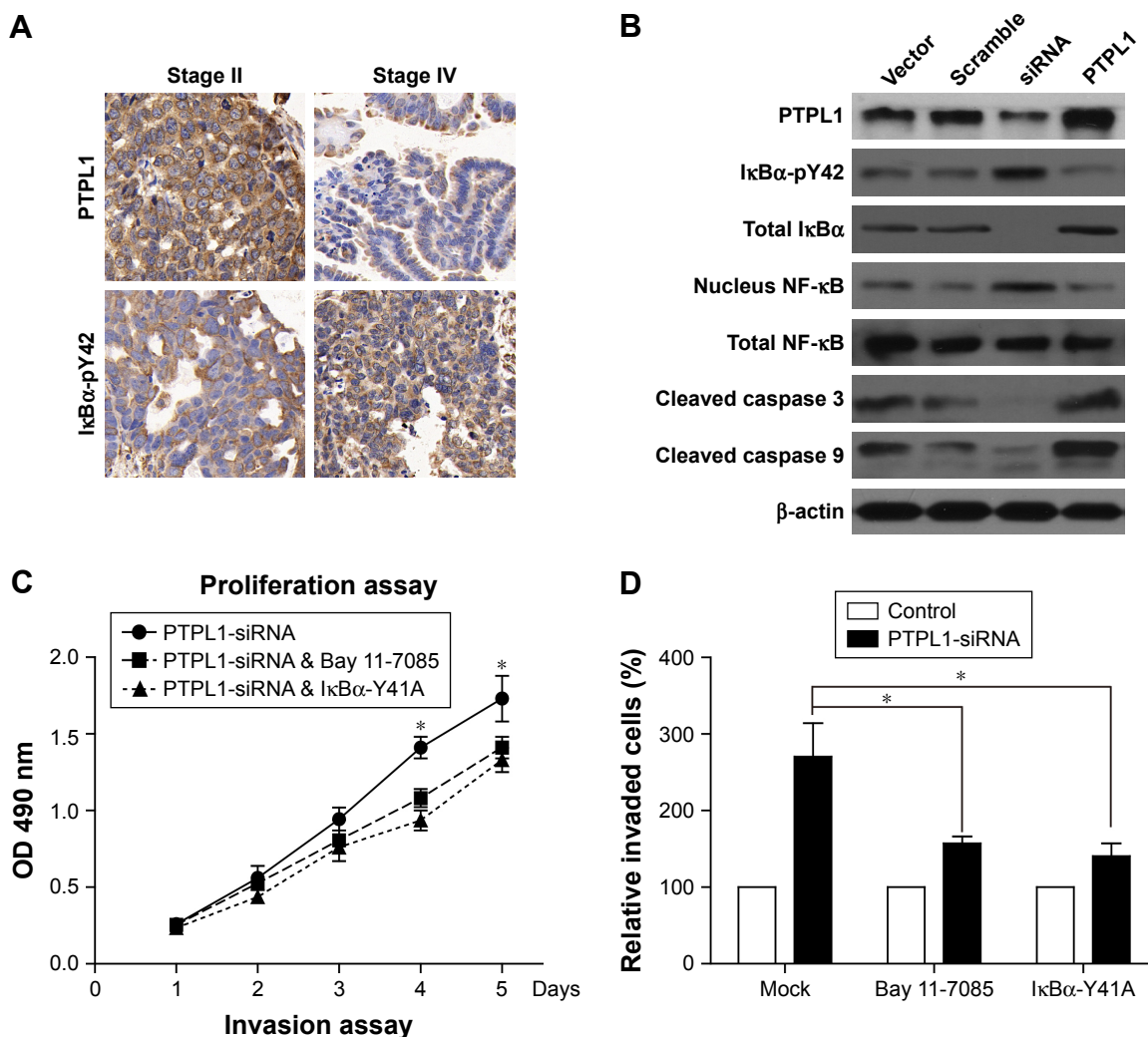


**Figure 4 (Continued)**



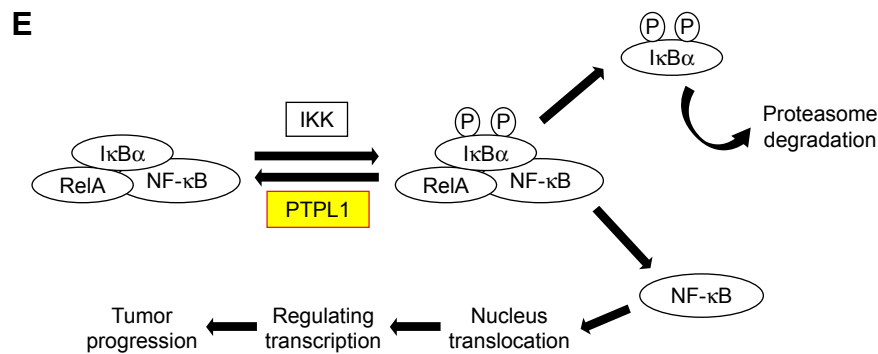


**Figure 4** Identification of I $\kappa$ B $\alpha$ -pY42 as a novel site recognized by PTPL1.

**Notes:** (A) Both PTPL1 and I $\kappa$ B $\alpha$  were predominantly localized in the cytoplasm. Importantly, I $\kappa$ B $\alpha$ -Y42 phosphorylation level was negatively correlated with the PTPL1 level. (B) In OV-90 cells transfected with PTPL1 plasmids, the phosphorylation on I $\kappa$ B $\alpha$ -Y42 was lower than that in control cells, which was consistent with the data from clinical samples. Subsequently, the phosphorylated I $\kappa$ B $\alpha$  protein underwent degradation, thereby released the NF- $\kappa$ B into the cell nucleus, as reflected by Western blot. By conducting the proliferation (C) and invasion (D) experiments, we found that the tumor-promoting effects of PTPL1-silencing were attenuated by I $\kappa$ B $\alpha$  inhibitor Bay 11-7085 or its tyrosine-alanine (Y42A) mutation. (E) The signaling axis of PTPL1-I $\kappa$ B $\alpha$ -pY42-NF- $\kappa$ B is shown in a schematic model. \* $p < 0.05$ .

**Abbreviation:** PTPL1, protein tyrosine phosphatase L1.

chief contributor to be recognized by PTPL1. Cellular results also demonstrated that dephosphorylation of I $\kappa$ B $\alpha$ -pY42 by PTPL1 can enhance the sequestering of NF- $\kappa$ B, thus reduce the transcription of oncogenic factors.

## Conclusion

Our results identified a prognostic role of PTPL1 in predicting the overall survival for surgical-treated HGSOc patients.

## Disclosure

The authors report no conflicts of interest in this work.

## References

- Siegel RL, Miller KD, Jemal A. Cancer statistics, 2018. *CA Cancer J Clin*. 2018;68(1):7–30.
- Singh N, Mccluggage WG, Gilks CB. High-grade serous carcinoma of tubo-ovarian origin: recent developments. *Histopathology*. 2017; 71(3):339–356.
- Przybycin CG, Kurman RJ, Ronnett BM, Shih I, Vang R. Are all pelvic (nonuterine) serous carcinomas of tubal origin? *Am J Surg Pathol*. 2010;34(10):1407–1416.
- Cohen JG, White M, Cruz A, Farias-Eisner R. In 2014, can we do better than CA125 in the early detection of ovarian cancer? *World J Biol Chem*. 2014;5(3):286–300.
- Vaughan S, Coward JI, Bast RC, et al. Rethinking ovarian cancer: recommendations for improving outcomes. *Nat Rev Cancer*. 2011;11(10): 719–725.
- Coleman RL, Monk BJ, Sood AK, Herzog TJ. Latest research and treatment of advanced-stage epithelial ovarian cancer. *Nat Rev Clin Oncol*. 2013; 10(4):211–224.
- Xiao K, Liu H. “Barcode” and Differential Effects of GPCR Phosphorylation by Different GRKs. *G Protein-Coupled Receptor Kinases*. 2016:75–120.
- Alonso A, Sasin J, Bottini N, et al. Protein tyrosine phosphatases in the human genome. *Cell*. 2004;117(6):699–711.
- Zhang J, Sapienza PJ, Ke H, et al. Crystallographic and nuclear magnetic resonance evaluation of the impact of peptide binding to the second PDZ domain of protein tyrosine phosphatase 1E. *Biochemistry*. 2010;49(43):9280–9291.
- Dromard M, Bompard G, Glondu-Lassis M, Puech C, Chalbos D, Freiss G. The putative tumor suppressor gene PTPN13/PTPL1 induces apoptosis through insulin receptor substrate-1 dephosphorylation. *Cancer Res*. 2007;67(14):6806–6813.
- Lee SH, Shin MS, Lee HS, et al. Expression of Fas and Fas-related molecules in human hepatocellular carcinoma. *Hum Pathol*. 2001;32(3): 250–256.
- Meinhold-Heerlein I, Stenner-Liewen F, Liewen H, et al. Expression and potential role of Fas-associated phosphatase-1 in ovarian cancer. *Am J Pathol*. 2001;158(4):1335–1344.
- Committee FC. Staging announcement: FIGO Cancer Committee. *Gynecol Oncol*. 1986;25:383–385.
- Mishima K, Nariai Y, Yoshimura Y. Etodolac, a selective cyclo-oxygenase-2 inhibitor, enhances carboplatin-induced apoptosis of human tongue carcinoma cells by down-regulation of FAP-1 expression. *Oral Oncol*. 2005;41(1):77–81.
- Liu H, Zhang Q, Li K, et al. Prognostic significance of USP33 in advanced colorectal cancer patients: new insights into  $\beta$ -arrestin-dependent ERK signaling. *Oncotarget*. 2016;7(49):81223–81240.
- Livak KJ, Schmittgen TD. Analysis of relative gene expression data using real-time quantitative PCR and the 2<sup>-</sup>(Delta Delta C(T)) Method. *Methods*. 2001;25(4):402–408.
- Birmie GD. *Subnuclear Components: Preparation and Fractionation*. London: Elsevier; 2016.
- Sorbi F, Progetto E, Turrini I, et al. Luteinizing Hormone/Chorionic Gonadotropin Receptor Immunohistochemical Score Associated with Poor Prognosis in Endometrial Cancer Patients. *Biomed Res Int*. 2018;2018:1–6.
- Wang J, Yao Y, Ming Y, et al. Downregulation of stathmin 1 in human gallbladder carcinoma inhibits tumor growth in vitro and in vivo. *Sci Rep*. 2016;6:28833.
- Zhang S, Balch C, Chan MW, et al. Identification and characterization of ovarian cancer-initiating cells from primary human tumors. *Cancer Res*. 2008;68(11):4311–4320.
- Tan W, Pan M, Liu H, Tian H, Ye Q, Liu H. Ergosterol peroxide inhibits ovarian cancer cell growth through multiple pathways. *Onco Targets Ther*. 2017;10:3467–3474.
- Hou S, Du P, Wang P, Wang C, Liu P, Liu H. Significance of MNK1 in prognostic prediction and chemotherapy development of epithelial ovarian cancer. *Clin Transl Oncol*. 2017;19(9):1107–1116.
- Baldwin AS. The NF- $\kappa$ B and I $\kappa$ B proteins: new discoveries and insights. *Annu Rev Immunol*. 1996;14(1):649–681.
- Viatour P, Merville MP, Bours V, Chariot A. Phosphorylation of NF- $\kappa$ B and I $\kappa$ B proteins: implications in cancer and inflammation. *Trends Biochem Sci*. 2005;30(1):43–52.
- Karin M, Ben-Neriah Y. Phosphorylation meets ubiquitination: the control of NF- $\kappa$ B activity. *Annu Rev Immunol*. 2000;18(1):621–663.

26. Révillion F, Puech C, Rabenoelina F, Chalbos D, Peyrat JP, Freiss G. Expression of the putative tumor suppressor gene PTPN13/PTPL1 is an independent prognostic marker for overall survival in breast cancer. *Int J Cancer*. 2009;124(3):638–643.
27. Scrima M, de Marco C, de Vita F, et al. The nonreceptor-type tyrosine phosphatase PTPN13 is a tumor suppressor gene in non-small cell lung cancer. *Am J Pathol*. 2012;180(3):1202–1214.
28. Ungefroren H, Kruse M-L, Trauzold A, et al. FAP-1 in pancreatic cancer cells: functional and mechanistic studies on its inhibitory role in CD95-mediated apoptosis. *J Cell Sci*. 2001;114(15):2735–2746.
29. Wieckowski E, Atarashi Y, Stanson J, Sato TA, Whiteside TL. FAP-1-mediated activation of NF-kappaB induces resistance of head and neck cancer to Fas-induced apoptosis. *J Cell Biochem*. 2007;100(1):16–28.

### OncoTargets and Therapy

## Publish your work in this journal

OncoTargets and Therapy is an international, peer-reviewed, open access journal focusing on the pathological basis of all cancers, potential targets for therapy and treatment protocols employed to improve the management of cancer patients. The journal also focuses on the impact of management programs and new therapeutic agents and protocols on

Submit your manuscript here: <http://www.dovepress.com/oncotargets-and-therapy-journal>

patient perspectives such as quality of life, adherence and satisfaction. The manuscript management system is completely online and includes a very quick and fair peer-review system, which is all easy to use. Visit <http://www.dovepress.com/testimonials.php> to read real quotes from published authors.

Dovepress